Dislocation dynamics analysis of hydrogen embrittlement in alpha iron based on atomistic investigations

Shinya Taketomi[1,*], Honami Imanishi[2], Ryosuke Matsumoto[2], Noriyuki Miyazaki[2]

[1] Department of Mechanical Engineering, Saga University, 840-8502, Japan
[2] Department of Mechanical Engineering and Science, Kyoto University, 606-8501, Japan
* Corresponding author: taketomi@me.saga-u.ac.jp

Abstract Hydrogen embrittlement is well known phenomenon in which hydrogen lowers the strength of materials. Hydrogen atoms show unique characteristics such as high diffusivity and low concentration in metals, so the direct observations of hydrogen effects on mechanical properties are still difficult. Nevertheless, experimental studies have been revealed many valuable results; HEDE (Hydrogen Enhanced Decohesion), HELP (Hydrogen Enhanced Localized Plasticity), HESIV (Hydrogen Enhanced Strain Induced Vacancy) and others have been proposed as a fracture mechanism of hydrogen embrittlement so far. However, the overview of the hydrogen embrittlement under various conditions is still unclear. In this study, we focus on the edge dislocation motion in the presence of hydrogen atom as one of the elementary process of hydrogen embrittlement in alpha iron. Our previous studies showed that the dislocation velocity increace (softening) occurs at lower hydrogen concentration and lower applied stress conditions. In contrast, dislocation velocity decrease (hardening) occurs at higher hydrogen concentration or higher applied stress conditions. Therefore, we performed the dislocation dynamics calculation around a crack tip based on the results obtained by our atomistic calculations. The results indicate that the hydrogen embrittlement mechanisms possibly change depending on boundary conditions (hydrogen concentration and applied stress intensity factor rate).

Keywords Hydrogen embrittlement, Dislocation dynamics, Atomistic simulation, Alpha iron

1. Introduction

Hydrogen embrittlement is well known phenomenon in which hydrogen lowers the strength of materials. Hydrogen atoms show unique characteristics such as high diffusivity and low concentration in metals, so the direct observations of hydrogen effects on mechanical properties are still difficult. Nevertheless, experimental studies have been revealed many valuable results; e.g. macroscopic hydrogen embrittlement fracture process, stress-strain relation and so on. HEDE (Hydrogen Enhanced Decohesion [1]), HELP (Hydrogen Enhanced Localized Plasticity [2]), HESIV (Hydrogen Enhanced Strain Induced Vacancy [3]) and others have been proposed as a fracture mechanism of hydrogen embrittlement so far. However, the overview of the hydrogen embrittlement under various conditions is still unclear. Here, we believe the evaluation of the elementary process can lead the understanding of whole image of hydrogen embrittlement, and we also believe the atomistic simulations can contribute the understanding of the hydrogen embrittlement, since the atomistic simulations show information in high resolution, and can easily exchange the boundary conditions (i.e. stress, temperature, hydrogen concentration). In this study, we focus on the edge dislocation motion in the presence of hydrogen atom as one of the elementary process of hydrogen embrittlement in alpha iron. Our previous studies [4-5] showed that the dislocation velocity increase (softening) occurs at lower hydrogen concentration and lower applied stress conditions. In contrast, dislocation velocity decrease (hardening) occurs at higher hydrogen concentration or higher applied stress conditions. These contradictive behaviors attribute the applied stress dependent competition between dislocation motion and hydrogen diffusion [4-5]. These atomistic studies, however, evaluated the individual dislocation motion due to the limitation of calculation cost. Therefore, in this study, we perform the dislocation dynamics calculations around a

crack tip based on the results obtained by our atomistic calculations for alpha iron, to evaluate the many-body effects of dislocations around a stress singularity field of a crack tip.

2. Methods of Dislocation Dynamics Analysis

In this study, we employ the analysis model as shown in Figure 1. In this model, one-dimensional edge dislocations are emitted from a mode II crack tip. The crack length is set as $2a$ and the dislocation source S is located at some finite distance of x_S from a crack tip. In this model, x_S is taken as 10^{-9} m, which corresponds to the order of the dislocation core, thus this dislocation source is regarded to be located at the crack tip from the viewpoint of continuum mechanics.

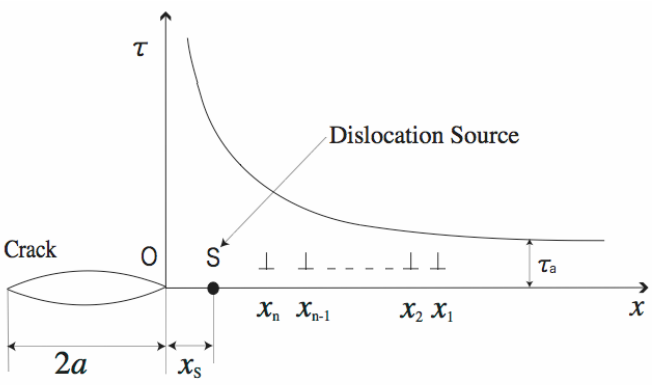

Figure 1. The model of dislocation emission and motion under the local stress field around crack tip

In this study, dislocation dynamics method which has been performed by A. T. Yokobori, Jr. et al. is adopted. Since the detailed analysis methods were reported in the previous papers [6-7], here we show the outline of the analysis method. As the stress distribution near a crack tip $\tau_a(x, t)$, the stress singularity near a crack tip was taken into account under a constant rate of stress application as follows:

$$\tau_a(x,t) = \dot{\tau}\sqrt{\frac{a}{x}} \quad , \tag{1}$$

where $\dot{\tau}$ is the increasing rate of stress application, t is time and x is the distance from the crack tip. The relationship between effective stress exerted on each dislocations moving along x direction and dislocation velocity are written for each individual dislocation in a coplanar array by the following equation:

$$v_i = \frac{\mathrm{d}x_i}{\mathrm{d}t} = Q\left(\Delta E_{\mathrm{dis}}\left(\tau_{\mathrm{eff},i}\right)\right)b \quad , \tag{2}$$

where, $Q(\Delta E_{\mathrm{dis}})$ is the frequency of dislocation motion with $1b$, ΔE_{dis} is the free energy barrier for dislocation motion and is a function of effective stress $\tau_{\mathrm{eff},i}$ and temperature T. b is the length of Burger's vector. The frequency of dislocation motion is determined by atomistic simulation as described later. Here, the effective stress exerted on the i th dislocation is written as follows:

$$\tau_{\mathrm{eff},i} = \dot{\tau}\sqrt{\frac{a}{x_i}} - A^*\left\{\frac{1}{2x_i} + \sum_{\substack{j=1 \\ i\neq j}}^{n}\left(\frac{1}{x_i + \sqrt{x_i x_j}} + \frac{1}{x_j - x_i}\right)\right\} \quad , \tag{3}$$

where, $A^* = \mu b/2\pi(1-\nu)$, μ is the shear modulus, ν is the Poisson's ratio, x_i is the distance of the i th dislocation from the crack tip. The first term is the macroscopic stress field around a crack tip by applied stress, the second and third terms are the image force of dislocations by the free boundary of

crack surface, and the fourth term is the interaction between other dislocations in the same dislocation array. Therefore the effective stress exerted on a dislocation source is written as follows:

$$\tau_{\mathrm{eff,s}} = \tau_{\mathrm{a}} \sqrt{\frac{a}{x_{\mathrm{s}}}} - A^{*}\left\{\frac{1}{2x_{\mathrm{s}}} + \sum_{j=1}^{n}\left(\frac{1}{x_{\mathrm{s}} + \sqrt{x_{\mathrm{s}}x_{j}}} + \frac{1}{x_{j} - x_{\mathrm{s}}}\right)\right\} \quad , \tag{4}$$

In this analysis, when the effective stress on dislocation source equals to the activation stress τ_{s}, then a new dislocation is introduced at the source.

3. Material Properties Obtained by Atomistic Simulations

3.1. Equilibrium Hydrogen Concentration

In order to evaluate the material properties (critical stress intensity factor for dislocation emission from mode II crack tip, dislocation velocity) in the presence of hydrogen, the realistic hydrogen concentration should be adopted. According to Sievert's law, the equilibrium concentration of hydrogen is proportional to $p^{1/2}$ and $\exp(-\Delta H/k_{\mathrm{B}}T)$, where p is the hydrogen gas pressure, ΔH is the heat of the solution, k_{B} is the Boltzman's constant and T is the temperature. Hirth [8] has reported the hydrogen concentration (atom fraction of hydrogen) for alpha iron under the gaseous hydrogen condition based on Sievert's law. The hydrogen atom stably exists at the tetrahedral site (T-site) within the non-deformed bcc structured alpha iron [9]. Therefore, the hydrogen occupancy at the T-site under thermal equilibrium conditions is given by equation (5) as a function of hydrogen gas pressure p (Pa) and temperature T (K).

$$\theta_{\mathrm{T-site}} = 0.9686 \times 10^{-6}\sqrt{p}\exp\left(-\frac{3440}{T}\right) \quad , \tag{5}$$

A close relation was also obtained by our evaluation using first-principles calculations [10]. Using the hydrogen occupancy at T-site, $\theta_{\mathrm{T\text{-}site}}$, the hydrogen occupancy at a specific trap site θ_i with hydrogen-trap energy $E^{\mathrm{Trap}}{}_i$ under thermal equilibrium condition is given by the following equation:

$$\frac{\theta_i}{1-\theta_i} = \frac{\theta_{\mathrm{T\text{-}site}}}{1-\theta_{\mathrm{T\text{-}site}}}\exp\left(\frac{E^{\mathrm{Trap}}{}_i}{k_{\mathrm{B}}T}\right) \quad , \tag{6}$$

where, the hydrogen-trap energy corresponds to the energy difference between the system with a hydrogen atom trapped at the specific trap site and the system with a hydrogen atom at a T-site within the non-deformed perfect lattice; this definition is the same as in our previous study [11]. To estimate the number of hydrogen atoms exist around the crack/dislocation at a thermal equilibrium conditions, these hydrogen occupancies are employed as same as our previous study[4,12].Using the equations (5) and (6), the hydrogen concentration around a {112}<111> edge dislocation (number of hydrogen atoms per unit length of dislocation line); C_{H} = 0.49 /nm under thermal equilibrium conditions can be realized at 300 K and 0.01 MPa hydrogen gaseous conditions. And C_{H} = 1.24 /nm can be realized at 300 K and 0.32MPa hydrogen gas.

3.2. Dislocation velocity

Dislocation motion is considered as stress-dependent thermal activation process. Our previous studies [4-5] showed that {112}<111> edge dislocation velocity as a function of applied shear stress via the estimation of energy barrier for dislocation motion. The dislocation velocity especially for the case of hydrogen free condition is written as following equation:

$$v = \nu_{\mathrm{d}}\exp\left(-\frac{\Delta E_{\mathrm{w/oH}}\, l^{*}}{k_{\mathrm{B}}T}\right)b \quad , \tag{7}$$

where, $\Delta E_{\mathrm{w/oH}}$ is the energy barrier for dislocation motion without hydrogen as a function of shear

stress, l^* is the length of edge dislocation line at the energy saddle point of the dislocation motion which are required to surmount for dislocation motion. k_B is the Boltzman's constant, T is the absolute temperature, ν_d is the attempt frequency of dislocation motion. On the other hand, in the presence of hydrogen, energy barrier landscape becomes complex depending on the correlation between the positions of dislocation and hydrogen atoms. According to the case analyses of the competition between dislocation motion and hydrogen atom diffusion, dislocation velocity vary from softening to hardening depends on applied shear stress [4] under the lower hydrogen concentration (C_H = 0.49 /nm). These results indicated that the softening attribute the decrease of energy barrier from 0b to 1b from the position of hydrogen atom, and hardening attribute the increase of energy barrier from 1b to 2b[4]. Moreover, the softening does not occur under high hydrogen concentration (C_H = 1.24 /nm) due to the increment of energy barrier from 0b to 2b[5]. These results of dislocation velocity obtained by atomistic simulations are employed as material properties for dislocation dynamics analyses. Here, the energy barrier is approximated as following function[13]:

$$\Delta E = A \cdot \left(1 - \tau / \tau_{ath}\right)^n \quad , \tag{8}$$

where, τ_{ath} is the athermal stress for dislocation motion, A and n are the fitting parameters. The parameters used in this study are shown in Table 1. Here, the dislocation velocity at higher hydrogen concentration condition (C_H = 1.24 /nm) is approximated as shown in Table 1. The energy barrier obtained in these results, however, neglected the contribution of the enthalpy effects. The effect of enthalpy is approximately considered as following equation[14], therefore the activation free energy for dislocation motion is written as:

$$\Delta E^{\mathrm{act-free}} = A\left(1 - T/T_m\right)\left(1 - \tau / \tau_{ath}\right)^n \quad , \tag{9}$$

where, T_m is the surface disordering temperature, and half of the melting temperature (T_m= 904 K) is adopted. In this study, the activation free energy as shown in equation (9) is employed as an energy barrier of dislocation motion, the obtained relationship between dislocation velocity and applied shear stress at 300 K are shown in Figure 2. At the low hydrogen concentration, dislocation velocity increase (compared with that in the absence of hydrogen) occurs when the applied stress is lower than 29 MPa, and decrease occur when the stress takes higher than 29 MPa. Moreover, applied stress takes over 81 MPa, dislocation velocity does not show the effect of hydrogen.

Table 1. Fitting parameters of the energy barrier for dislocation motion

	n	τ_{ath}	A
Hygrogen free	1.48	660	0.0821
C_H=0.49 /nm ($\tau \leqq$28MPa)	1.41	680	0.0795
C_H=0.49 /nm ($\tau \geqq$81MPa)	1.48	660	0.0821
C_H=1.24 /nm	1.41	680	0.0795

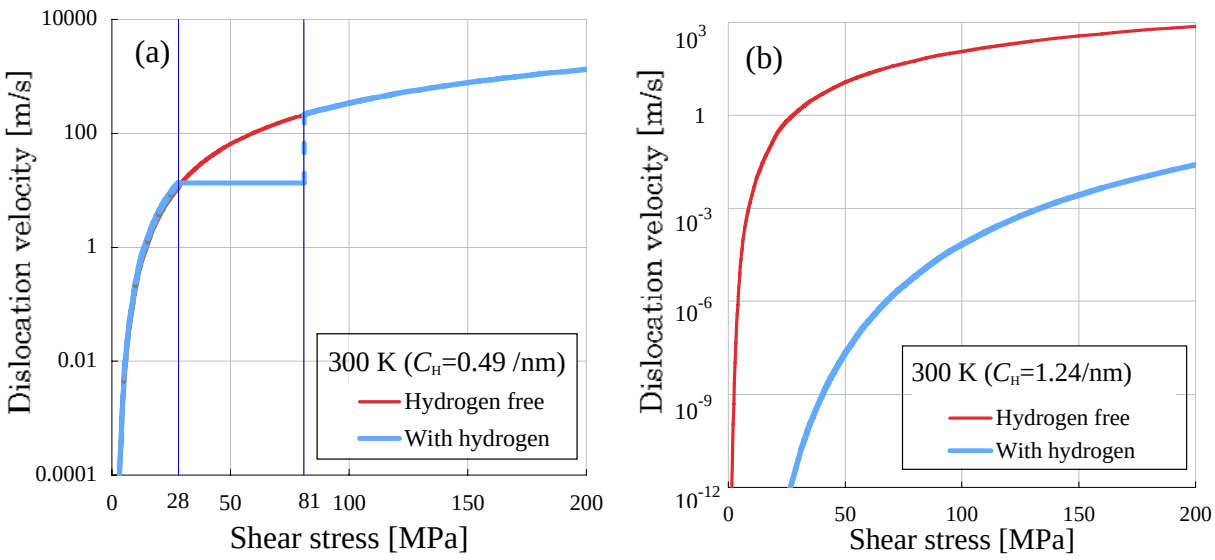

Figure 2. Relationship between dislocation velocity and shear stress at 300 K; (a) low hydrogen concentration condition(C_H = 0.49 /nm), (b) high hydrogen concentration condition(C_H = 1.24 /nm)

3.3. Dislocation Emission from Crack Tip

The activation stress of dislocation source to emit a new dislocation is determined as follows:

$$\tau_s = \frac{K_{IIC}}{\sqrt{\pi x_s}} \quad , \tag{10}$$

where, K_{IIC} is the critical stress intensity factor for edge dislocation emission from a mode II crack tip. The atomistic analyses showed that increasing the hydrogen concentration, the K_{IIC} value decrease in alpha iron[12]. We employ these relationships and the critical stress intensity factors used in this study are shown in Table 2. It clearly shows that the dislocation emission is enhanced in the presence of hydrogen.

Table 2. Critical stress intensity factor for dislocation emission

	Hydrogen free	C_H = 0.49 [/nm]	C_H = 1.24 [/nm]
K_{IIC} [MPam$^{1/2}$]	0.443	0.440	0.430

4. Analysis Results of Dislocation Dynamics

4.1. Low Hydrogen Concentration (C_H = 0.49 /nm)

The correlation between applied stress intensity factor rate ($\dot{K} = \dot{\tau}\sqrt{\pi a}$ MPam$^{1/2}$/s) and the distance of leading dislocation (first emitted dislocation) from a crack tip (i.e. the size of the plastic zone) at the specific stress intensity factor (K = 0.589 MPam$^{1/2}$) is shown in Figure 3 (a). It reveals that the size of the plastic zone becomes large in the presence of hydrogen, which is considered to attributes the increase of dislocation velocity (τ < 29 MPa in Figure 2), and the enhancement of dislocation emission (in Table 2). On the other hand, at the high applied stress intensity factor rate conditions, the size of plastic zone becomes small compared with that in the presence of hydrogen. It is considered to attributes the increase of effective stress exerted on each dislocation near the crack tip (τ > 29 MPa in Figure 2). Figure 3 (b) shows the number of emitted dislocations. This figure shows

the increase of the number of emitted dislocations at lower applied stress intensity factor rate, however, it also decrease at high stress intensity factor rate conditions. The distributions of dislocations at several applied stress intensity factor rate (A) $\dot{K}$=0.56 MPam$^{1/2}$/s, (B) $\dot{K}$=56 MPam$^{1/2}$/s are shown in Figure4. In this figure, we considered that dislocation motion is softened when the exerted effective stress at each dislocation takes below 29 MPa. And the hardening is also considered to occur when the effective stress takes between 29 to 81 MPa. At this hydrogen concentration, both the size of plastic deformation zone and the number of emitted dislocations increase due to the softening effect at lower applied stress intensity factor rate conditions. However the hardening becomes dominant at higher applied stress intensity factor rate. This result indicate that the local hardening near the crack tip can occur even the macroscopic softening conditions, and thus the plastic deformation is supposed to be complex in these conditions.

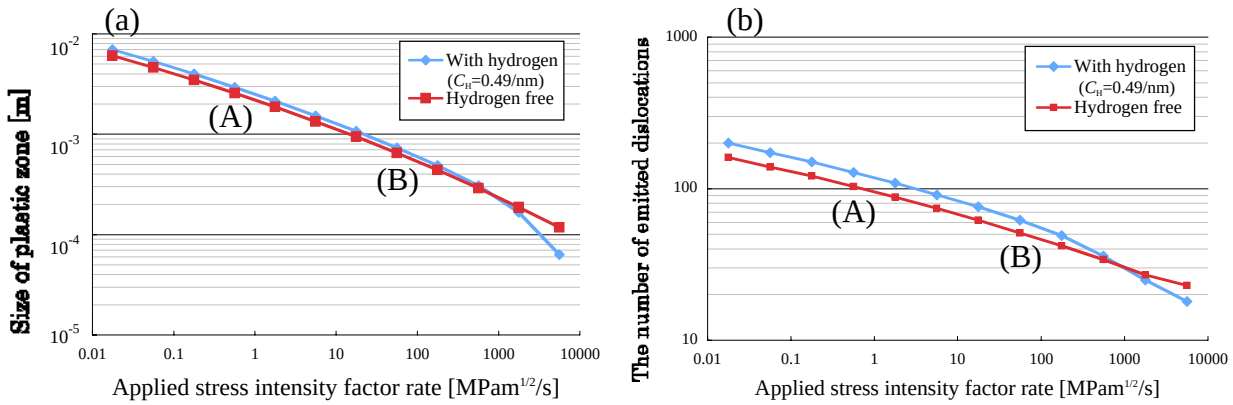

Figure 3. Correlation between the applied stress intensity factor rate and;
(a): distance of first emitted dislocation, (b): the number of emitted dislocations

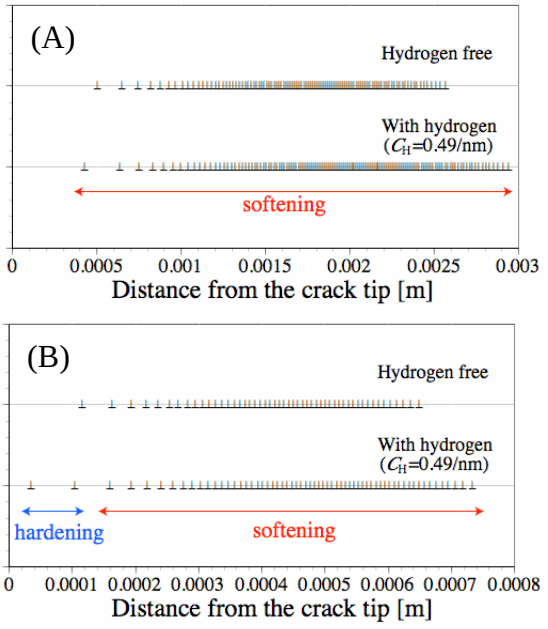

Figure 4. Dislocation distribution around a crack tip at the stress intensity factor rate of
(A): 0.56 MPam$^{1/2}$/s, (B): 56 MPam$^{1/2}$/s

4.2. High Hydrogen Concentration (C_H = 1.24 /nm)

The correlation between applied stress intensity factor rate and the distance of leading dislocation from a crack tip (i.e. the size of the plastic zone) at the specific stress intensity factor (K = 0.589 MPam$^{1/2}$) at high hydrogen concentration is shown in Figure 5(a). The size of plastic zone at this hydrogen concentration becomes typically small. The correlation between applied stress intensity factor rate and the number of emitted dislocation is shown in Figure 5(b). Although, the dislocation emission is enhanced at this hydrogen concentration, the number of emitted dislocations typically decreases. The dislocation distributions are also shown in Figure 6. These results indicate that only hardening can occur at this high hydrogen concentration conditions.

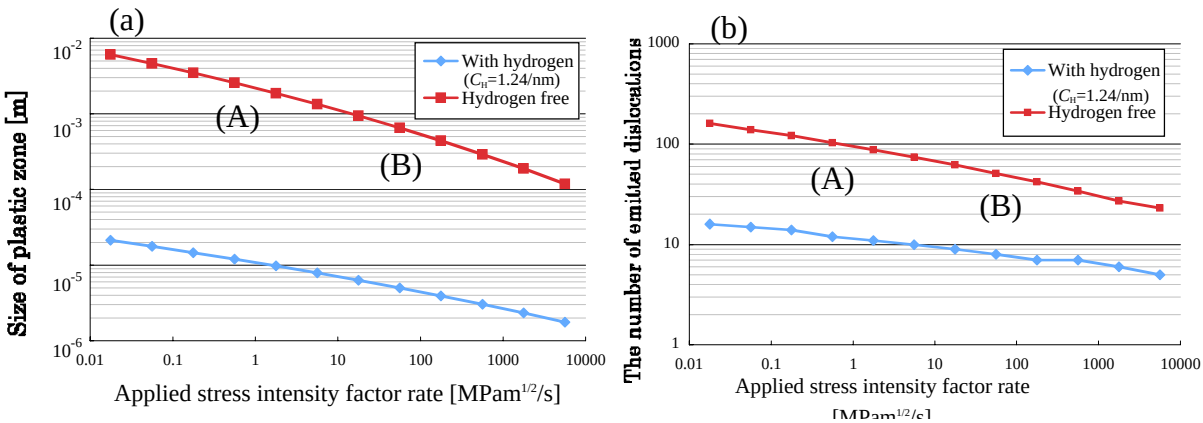

Figure 5. Correlation between the applied stress intensity factor rate and;
(a): distance of first emitted dislocation, (b): the number of emitted dislocations

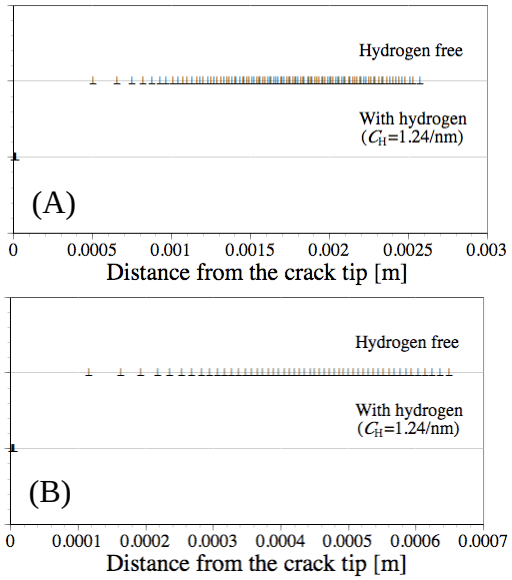

Figure 6. Dislocation distribution around a crack tip at the stress intensity factor rate of
(A): 0.56 MPam$^{1/2}$/s, (B): 56 MPam$^{1/2}$/s

4.3. Hydrogen Effects on Fracture Mechanisms

Dislocation slip behavior around a crack tip is enhanced at low hydrogen concentration and low stress intensity factor rate conditions, which result in softening. At the high hydrogen concentration

conditions, on the other hand, only hardening occur independent of applied stress intensity factor rate conditions. Based on these analyses results mentioned above, softening around a crack tip occur at the low hydrogen concentration and the low applied stress intensity factor rate conditions. Therefore, the amount of plastic deformation around a crack tip is supposed to increase and yield in the fracture mechanism of HELP and/or HESIV so far. However, at the high hydrogen concentration or the high applied stress rate conditions, hardening around a crack tip lead the brittle type fracture, HEDE so far. The schematic illustration of these relationships of hydrogen embrittlement mechanisms depending on environmental and mechanical conditions are shown in Figure 7.

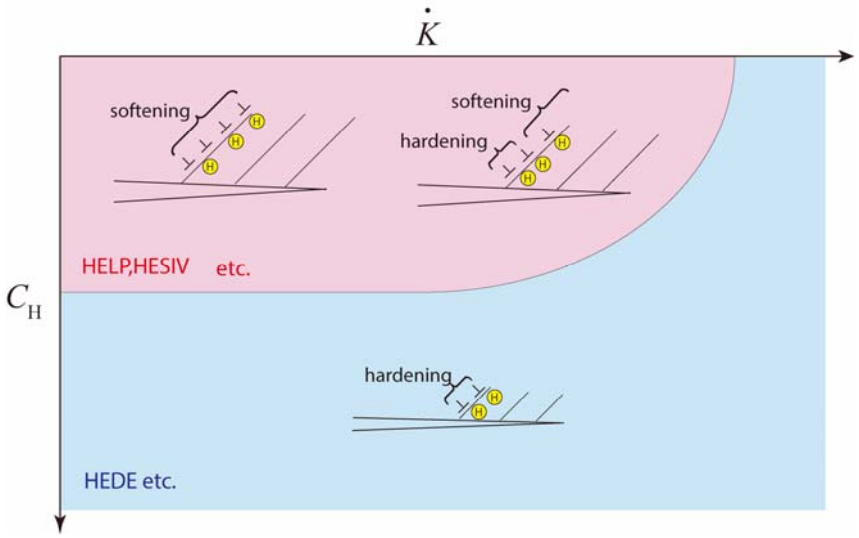

Figure 7. Hydrogen embrittlement fracture mechanisms for different hydrogen concentration and applied stress intensity factor rate conditions

5. Conclusion

In this study, we performed the dislocation dynamics calculation around a crack tip based on the results obtained by atomistic calculations. The results indicate that the hydrogen embrittlement mechanisms possibly change depending on boundary conditions (hydrogen concentration and applied stress intensity rate).

Acknowledgements

The author would like to acknowledge Prof. A.T. Yokobori,Jr.(Tohoku Univ.) for useful discussions and suggestions.

References

[1] R.A. Oriani, H.Josephic, Acta Metallurgica, 22 (1974) 1065–1074.
[2] C.D. Beachem, Metall. Trans. 3 (1972) 437–451.
[3] M. Nagumo, Mater. Sci. Tech. 20 (2004) 940–950.
[4] S. Taketomi, R. Matsumoto, N. Miyazaki, J. of Mat. Res., 26, 10 (2011) 1269–1278.
[5] S. Taketomi, R. Matsumoto, N.Miyazaki, Proc. of 2012 Hydrogen Conference, (2012) (submitted).
[6] A.T. Yokobori, Jr., T. Iwadate, T. Isogai, Acta Metall. Mater., 41 (1993) 1405–1411.
[7] A.T. Yokobori, Jr., T. Iwadate, T. Isogai, ASTM STP1207 (1994) 464–477.
[8] J.P. Hirth, Metall. Trans. A. 11A (1980) 861–890.

[9] R. Matsumoto, Y. Inoue, S. Taketomi, N. Miyazaki, Scripta Materialia, 60 (2009) 555–558.
[10] Y. Sakagami, R. Matsumoto, D. Alfè, S. Taketomi, T. Enomoto and N. Miyazaki, Transactions of the Materials Research Society of Japan ,37 (2012) 1–6.
[11] S. Taketomi, R. Matsumoto, N. Miyazaki, Acta Materialia, 56 (2008) 3761–3769.
[12] S. Taketomi, R. Matsumoto, N. Miyazaki, Journal of Mechanical Science, 52 (2010) 334–338.
[13] S. Izumi, S. Yip, Proc. of MD sympo. (2008) 1–4. (in Japanese)
[14] D.H. Warner, W.A. Curtin, Acta Materialia, 57 (2009) 4267–4277.